

sEMG-based Human-in-the-Loop Control of Elbow Assistive Robots for Physical Tasks and Muscle Strength Training

Roberto Meattini, Davide Chiaravalli, Gianluca Palli and Claudio Melchiorri

Abstract—In this article we present a sEMG-driven human-in-the-loop (HITL) control designed to allow an assistive robot produce proper support forces for both *muscular effort compensations*, i.e. for assistance in physical tasks, and *muscular effort generations*, i.e. for the application in muscle strength training exercises related to the elbow joint. By employing our control strategy based on a Double Threshold Strategy (DTS) with a standard PID regulator, we report that our approach can be successfully used to achieve a target, quantifiable muscle activity assistance. In this relation, an experimental concept validation was carried out involving four healthy subjects in physical and muscle strength training tasks, reporting with single-subject and global results that the proposed sEMG-driven control strategy was able to successfully limit the elbow muscular activity to an arbitrary level for effort compensation objectives, and to impose a lower bound to the sEMG signals during effort generation goals. Also, a subjective qualitative evaluation of the robotic assistance was carried out by means of a questionnaire. The obtained results open future possibilities for a simplified usage of the sEMG measurements to obtain a target, quantitatively defined, robot assistance for human joints and muscles.

I. INTRODUCTION

An assistive robot is a robot that interacts cognitively and physically with a user in order to assist her motion and/or joint torque generation [1]. The usage of this kind of robotic systems can be classified with respect to two main applications: human power augmentation and rehabilitation [1]. Despite the different kinematic configurations and implementations of this kind of robotic systems, the regulation of the behaviour of assistive robots is a very challenging problem in the research community, and the design of appropriate control strategies is still an open and common issue, being the user at close interaction with the robotic device in a general framework known as human-in-the-loop (HITL) [2]. Moreover, the assistive system should also be able to help a user during both the execution of physical tasks (i.e., partially or totally compensating the human effort) and muscle strength training exercises (i.e., providing proper resistive forces in order to impose a specific human effort generation.) Indeed, physical therapy of muscles concerns with restoring, preventing or slowing deterioration of motor functioning. In addition to neuro-motor diseases rehabilitation [3], therapy interventions are well known to be effective also for the prevention of muscle weakness attributable to

aging and long-period immobilizations due to hospitalization or admission to an intensive care unit [4]. In this relation, muscle strength training is the core intervention [5], defined as repetitive contractions of individual muscles against a resistive force [6]. In particular, muscle strength training is also applied for the so called *prehabilitation* [7], that is, in preparation for anticipated hospitalization/limb inactivity, such that an individual would be more likely to withstand future muscle weakening.

To achieve a more effective robotic assistance, several researchers have studied methods to obtain accurate human joint torque estimations based on sEMG measurements [8]. However, such kind of estimations have to deal with complex training procedures and limiting computational power requirements, making these systems arduously usable outside laboratories [9]. In our work, we propose to directly use the (filtered) muscle sEMG activity within the assistive control loop, avoiding imprecise data-driven predictions of joint torques and leaning on the adaptation capacity of the human motor control system to external physical assistance. In literature, there are a series of sEMG-driven robot controls recognized as assist-as-needed methods [10]: in [11] an interface to control exoskeletons based on a biomechanical model of the human body was proposed and experimented; [9] tested a control method characterized by the application of a proportional gain to the sEMG signal, without the possibility to impose a predetermined level of assistance; [12] performed an identification of a bio-inspired musculoskeletal model to control the exoskeleton assistance; an assist-as-needed controller was proposed in [13], using a model predictive control approach to estimate human joint torques to provide the correct amount of assistance. Robot-based muscle activity minimization have been considered in a number of studies, however reporting for limiting time-demanding procedures [14], results restricted to numerical simulation scenarios [15], or robotic assistance evaluation limited to an *a posteriori* analysis without the presence of a sEMG-driven closed loop. Differently, in this article, we propose an sEMG-based, closed loop, HITL control in which specific assistance objectives can be demanded to an assistive robot, in order to produce interaction forces for both physical tasks and muscle strength training related to the elbow joint. In our previous work [16], we provided an early evaluation about the possibility of limiting the biceps' activity to a desired maximum value, thanks to a closed-loop sEMG-driven control of an elbow support device. However, such previous study was still based on the usage of a muscular model for torque estimations, and was restricted to a simple compen-

The authors are with DEI – Dept. of Electrical, Electronic and Information Eng., Univ. of Bologna, Italy; e-mail: roberto.meattini2,davide.chiaravalli2,gianluca.palli, claudio.melchiorri@unibo.it

This research was partially supported by the European Commission's Horizon 2020 Framework Programme with the project REMODEL - Robotic technologies for the manipulation of complex deformable linear objects - under grant agreement No 870133.

sation of the biceps effort in static conditions. Distinctly, in this article we outline a series of advancements, since the objective of the present work is to introduce a joint-torque-estimation-free control and to demonstrate its effectiveness in allowing both dynamic human effort compensation and effort generation, for biceps and triceps. To this aim, we report the results of a concept validation experiment, in which four healthy subjects were involved in specific robot-assisted physical and muscle strength training tasks. The main goal of the experiment was to show the feasibility of the designed control strategy, therefore with a focus on evaluating system behaviour criteria rather than statistical significances. In this regard, note that the objective of the muscle strength training tasks was to demonstrate the feasibility of the control in providing a resistive force to generate a specified level of muscle activity – in accordance to the founding concept of muscle strength training – whereas a clinical testing with a larger population including impaired subjects will be devoted to a dedicated future work. Finally, also a questionnaire for a qualitative evaluation was submitted to the participants of the experiments, allowing to report a subjective assessment of perceived exertion and usefulness/usability of the robotic assistance.

II. METHODS AND TOOLS

A. sEMG Signal Acquisition

The sEMG signals were acquired by means of the biopotentials acquisition board *Cerebro* [17], composed by a high-performance Analog Front End (AFE) connected with an ARM Cortex M4 Microcontroller – the reader may refer to [17] for further details about this board. In this application, the data were sampled at 1 kHz and transmitted via Bluetooth to the control computer. Two couples of low cost differential electrodes were placed on the dominant upper arm of the subjects, in proximity of the biceps brachii and triceps brachii (long head) muscle bellies. Note that a processing procedure was applied to the raw sEMG signals, based on our previous work [16] and composed by: (i) a 50Hz notch filter, (ii) a 20Hz high-pass filter and, finally, (iii) a Root Mean Square (RMS) evaluator computing on a 200ms running window.

B. sEMG-based HITL Control for Elbow Assistive Robots

The sEMG-based HITL control interface proposed in this work is thought to provide assistance to the elbow joint flexion/extension-related muscular activity. Since we want to regulate an assistive robot in order to realize both target muscular *effort compensation* and *effort generation* during physical and muscle strength training tasks, the goal of the controller is specified in a twofold fashion:

- (i) to allow the robot provide a *support* force to the users' forearm such to impose an arbitrary *upper limit* to the biceps' and triceps' sEMG, during physical tasks characterized by flexion/extension actions;
- (ii) to allow the robot provide a *resistive* force to the users' forearm in such a way to impose an arbitrary *lower limit* to the biceps' or triceps' sEMG activity, based on the user needs (i.e., muscle strength training.)

1) *Description of the sEMG-based Control:* In Fig. 1, a block diagram of the proposed control scheme is illustrated. With relation to this figure, it is possible to observe how the robot assistive force F_{app} – applied to the user's forearm as shown in Fig.4 – is provided in accordance to a particular sEMG-driven control loop. Also, in Fig. 1, F_L represents the force that the forearm has to apply for some specific task involving only the elbow joint. In order to generate F_{app} , two specific Double Threshold Strategy (DTS_i) blocks are present, one related to the sEMG measurement from the biceps E_b and the other related to the triceps' sEMG E_t . The outputs of DTS_b and DTS_t are then modulated by the “Co-contraction Handler” block, in order to deal with the possibility of biceps-triceps co-activations and, thereafter, the output u of the Co-contraction Handler block is provided to a PID regulator in order to generate the reference value F_{robot} for the robot internal force controller. In the following, the subscript $i = \{b, t\}$ will indicate the biceps and triceps muscles, respectively.

In relation to Fig. 1, the behaviour of each DTS block is based on the exploitation of two threshold values, $T_{1,i}$ and $T_{2,i}$. The role of these thresholds is to specify certain levels of the sEMG activity such that: (i) $T_{2,i}$ is used to activate the robot assistance (see details in the following, referring to the finite state machine of Fig. 2 and the related “Activated Threshold Tracking” state S_2); (ii) $T_{1,i}$ is used, at the same time, as reference value for the computation of the sEMG error for the closed-loop control (refer to eq. (1), Fig. 1) and to deactivate the robot assistance once the target muscular effort compensation/generation has been achieved (refer in the following to Fig. 2 and the related “Deactivated Threshold Tracking” state S_1 .) The sEMG error signal r_i is then given by:

$$r_i = T_{1,i} - E_i, \quad (1)$$

where, as mentioned above, E_i is the sEMG signal from the biceps/triceps muscles. In this relation, the output of the DTS block is given in accordance with the two Finite State Machine (FSM) reported in Fig. 2, where: the state S_1 represents the “Deactivated Threshold Tracking” state and S_2 the “Activated Threshold Tracking” state, according to which the output of DTS_i is given as:

$$y_i = \begin{cases} 0, & \text{if FSM's state is } S_1 \\ r_i, & \text{if FSM's state is } S_2 \end{cases}. \quad (2)$$

In practice, the output of DTS_i is simply a modulation of the sEMG error r_i in accordance to the FSM of Fig. 2 – it follows that the unit of measurement of y_i is the same as for r_i , i.e. millivolt (mV). As an explanatory example, the behaviour of y_i for the biceps muscle is provided in Fig. 3, in response to a fictive sEMG input artificially generated. In particular, as described in Fig. 2, two possible assistance modalities can be selected by the user and/or the experimenter: (i) the *effort compensation functioning* and (ii) the *effort generation functioning*. As summarized in Tab. I for a better readability, these two assistance modalities can be enabled according to a proper selection of $T_{1,i}$ and $T_{2,i}$ combinations. In the

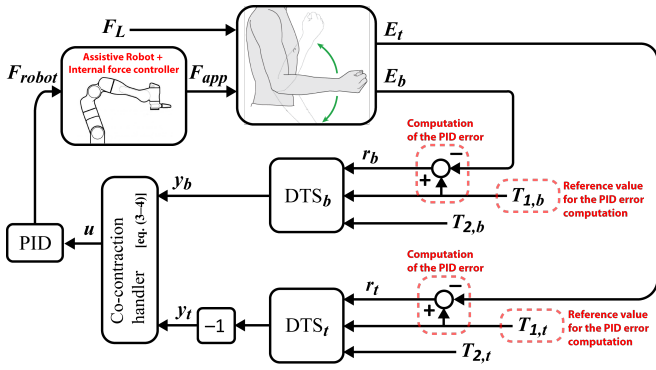


Fig. 1. Block diagram of the proposed sEMG-based control. In the figure, the variables E_i represents the sEMG signal, $T_{1,i}$ and $T_{2,i}$ the threshold values for the DTS_i block and related FSM (refer also to Fig. 2), r_i the sEMG error signal, y_i the modulation of r_i according to the DTS_i 's logic, u the modulation of y_i according to eqs. (3–4), F_L the force required to the human forearm by the task, F_{robot} the reference force for the robot and F_{app} the assistive force applied by the robot to the user – with $i = \{b, t\}$ indicating biceps and triceps. Please refer also to Fig. 3 for an explanatory (fictive) example of the behaviour of the variable y_i and u .

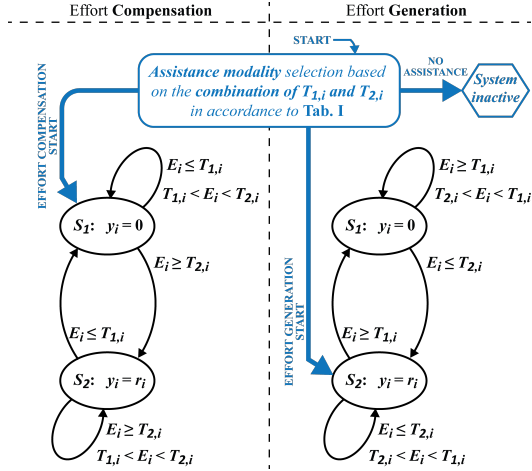


Fig. 2. FSM logic of the DTS_i block of Fig. 1. The state S_1 represents the “Deactivated Threshold Tracking” state and S_2 the “Activated Threshold Tracking” state, according to which the output of DTS_i is given by eq. (2). For the combination of $T_{1,i}$ and $T_{2,i}$ refer to Tab. I. (with $i = \{b, t\}$ indicating biceps and triceps.) For the meaning of the other variables refer to the caption of Fig. 1 and to Sec. II-B.

following, a detailed explanation of the sEMG-driven control behaviour for the effort compensation and effort generation functioning is provided.

Effort Compensation for Physical Tasks: In this scenario, a force $F_L \neq 0$ has to be generated by the forearm (see Fig. 4 and 1.) During these types of assistance functioning, the related transition logic of DTS_i is illustrated on the left side of Fig. 2, determining the inputs of the Co-contraction Handler block according to Eq. (2). Co-contraction Handler, in turn, provides the input for the PID regulator as

$$u = \begin{cases} y_t, & \text{if } y_b = 0 \\ y_b, & \text{otherwise} \end{cases} \quad (3)$$

In this way, the effort compensation can be provided for both the biceps and triceps, which are the prime elbow-related movers. Indeed, during a physical task which requires the forearm to produce a force $F_L > 0$ (alternatively, $F_L < 0$),

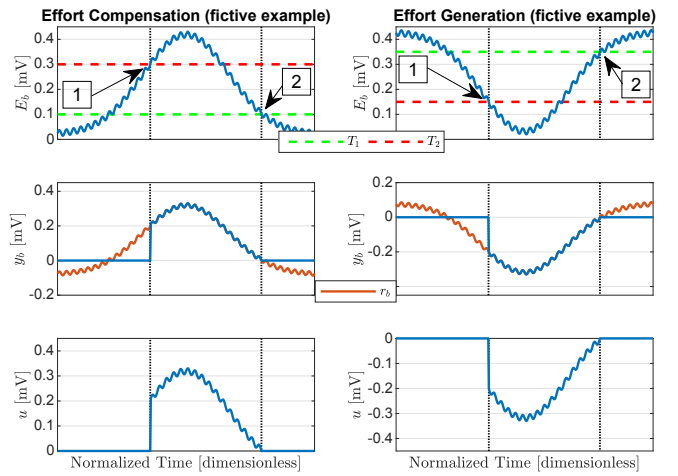


Fig. 3. Example of the behaviour of the variables y_b (middle row) and u (bottom row) – appearing in Fig. 1 and eq. (2–4) – with respect to a fictive biceps’ sEMG input E_b (top row). E_b was artificially generated as a sinusoid with a Gaussian-curve-modulated mean value in order to better show the behaviour of y_i . r_b is the sEMG error signal (eq. (1)); T_1 and T_2 are the input threshold values of the DTS block. Finally, in the top row, the number “1” arrow indicates the instant of the transition from the state S_1 to the state S_2 in the FSM of Fig. 2, whereas the number “2” arrow the transition from the state S_2 to the state S_1 .

E_b (E_t) will increase and surpass the threshold $T_{2,b}$ ($T_{2,t}$) activating the output y_b (y_t) of the DTS_b (DTS_t) block (see Fig. 4–2). This determines F_{app} in accordance to the reference F_{robot} provided by the PID to the robot’s internal force controller. In this way, E_b (E_t) will decrease thanks to the robot’s F_{app} action, until E_b (E_t) itself reaches the (lower) threshold $T_{1,b}$ ($T_{1,t}$) – therefore, realizing a transition from the state S_2 to the state S_1 of the FSM, i.e., realizing $y_i = 0$ in accordance to Eq. 2 and Fig. 2. Note that this is possible thanks to the adaptation of the user’s Central Nervous System (CNS) to the support provided by the robot. Furthermore, it is important to consider the possibility that both biceps’ and triceps’ sEMG activity can exceed the threshold $T_{2,i}$, i.e. in case of voluntary co-contraction. In the context of this study, our primary goal was to avoid the unpredictability of the assistance during co-contraction. Indeed, during the effort compensation functioning, the sEMG-driven control is designed to provide the correct assistance both for biceps and triceps without the need to modify the threshold combination (i.e., without changing assistance modality, see also Tab. I), *except* in the case of co-contraction. To avoid this situation, the Co-contraction Handler block acts in order to “disable” the DTS_t block, considering therefore only the sEMG activity of the biceps (i.e., $u = y_b$), according to Eq. (3). In this way, in case of biceps-triceps co-contraction, we deliberately provide assistance only to the biceps, avoiding unplanned robot forces that could even be dangerous for the user safety. In any case, as expected, during our experiment (see Sec. III) no relevant co-contractions were detected in the subjects, because of smooth motions and predetermined environment/objectives. However, since in general the possibility of co-contraction exists (voluntarily, or due to external non-predictable events), we will consider in depth the aspect of co-contraction in future dedicated studies, being it out of

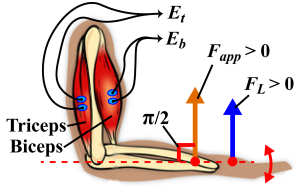


Fig. 4. Qualitative scheme of the forces applied on the forearm and the sEMG acquired from the biceps and triceps. E_i represents the sEMG signal, F_L the force required to the human forearm by the task, and F_{app} the assistive force applied by the robot to the user – with $i = \{b, t\}$ indicating biceps and triceps.

TABLE I

COMBINATIONS OF THRESHOLDS FOR THE ASSISTIVE MODALITIES.

Threshold Values	Assistance Modality
$T_{1,b} > T_{2,b}$	Effort Generation (Biceps, see Eq. (4))
$T_{1,t} < T_{2,t}$	Effort Compensation (both biceps and triceps)
$T_{1,b} < T_{2,b}$	Effort Generation (Triceps, see Eq. (4))
$T_{1,t} > T_{2,t}$	No Assistance/System Inactive
$T_{1,t} = T_{2,t}$	No Assistance/System Inactive
$T_{1,b} = T_{2,b}$	No Assistance/System Inactive

the aim of this work.

Effort Generation for Muscle Strength Training: Referring also to Fig. 4 and 1, in this situation we have $F_L = 0$, since it is not required to the user to apply target forces in order to accomplish a task goal. In this case, the aim is to allow the user generate a target muscle activity with her biceps or triceps during elbow motions, exploiting sEMG-driven robotic assistance. The FSM logic of the DTS_i block related to this kind of functioning is reported in the right side of Fig. 2. The behaviour of the Co-contraction Handler block is given such that its output corresponds to

$$u = \begin{cases} y_b, & \text{if } T_{1,b} > T_{2,b} \\ y_t, & \text{if } T_{1,t} > T_{2,t} \wedge T_{1,b} < T_{2,b} \end{cases} \quad (4)$$

According to this equation, the effort generation is provided for the biceps muscle when $T_{1,b} > T_{2,b}$ (i.e., *biceps strength training*); conversely, if $T_{1,t} > T_{2,t}$, the effort generation will be related to the triceps muscle (i.e., *triceps strength training*) – refer also to Tab. I. Indeed, during the biceps effort generation (alternatively, triceps effort generation) case, if E_b (E_t) is lower then the threshold $T_{2,i}$, the output y_b (y_t) of the DTS_b (DTS_t) block will be activated. This causes that the robot will apply a resistive force F_{app} on the user’s forearm in such a way that the signals E_b (E_t) will increase until it reaches the (higher) threshold $T_{1,b}$ ($T_{1,t}$). Finally note that, in this case of effort generation assistance, the Co-contraction Handler block just ensures that during a biceps or triceps strength training case, only the related biceps or triceps sEMG activity is taken into account, respectively.

C. Assistive Robotic Setup and Control

In order to test the proposed HITL control in a robotic assistive scenario with multiple subjects (see, in the following, Sec. III), we used the Franka Emika Panda robot [18] (see Fig. II-C), a recently commercialized 7-degrees-of-freedom (DoF) manipulator, which is gaining popularity in the robotic

community for its high usability and low price among the torque controlled robots. Furthermore, in order to transmit the robot assistive force to the user’s forearm (in accordance to Fig. 4), an end-effector for the Franka Emika Panda have been specifically designed and realized by 3D-printing. In Fig. 5(a), it is possible to observe the end-effector worn by a subject: it is composed of an upper and lower part (internally coated with a layer of anti-allergenic latex) that can be fixed to the user’s forearm by straps fastening. Importantly, solidly connected to the top part of the end-effector, it is present a flange that permits a robust attachment to the Panda’s terminal flange (Fig. 5(b),5(c),5(d).)

With regard to the generation of the assistive force F_{app} with the Franka Emika Panda – in accordance to the block “Assistive robot (force control)” of the overall HITL control of Fig. 1 – the goal was to implement a robot force control exploiting the already available manipulator’s low level torque controller in order to generate: (i) a robot gravity compensation and (ii) the application of a force \vec{F}_{app} perpendicular to the forearm of the subjects (in accordance with Fig. 4) such that its module tracks the reference force module F_{robot} required by the sEMG-controller. To this purpose, let’s consider the dynamic model of the $n = 7$ DoF manipulator Franka Emika Panda, described by [19]

$$M(q)\ddot{q} + C(q, \dot{q})\dot{q} + g(q) = \tau + J^T(q)\vec{F}_h^R \quad (5)$$

where $q \in \mathbb{R}^n$ is the joint vector, $M(q) \in \mathbb{R}^{n \times n}$ the inertia matrix, $C(q, \dot{q}) \in \mathbb{R}^{n \times n}$ the Coriolis and centrifugal effect matrix and $g(q) \in \mathbb{R}^n$ the gravitational term. A detailed description of the derivation and evaluation of the dynamical parameters of Eq. (5) can be found in [19]. Note that, in practice, the Franka Panda robot automatically provides in real-time the evaluation of all the dynamic parameters required for the model, and therefore we didn’t need to directly evaluate the dynamic parameters, since they were already provided by the robotic system. Moreover, considering the case with the manipulator attached to the human forearm, in Eq. (5) $\vec{F}_h^R \in \mathbb{R}^6$ represents the external wrench – expressed in robot base frame coordinates – applied by the subject by means of the previously described end-effector, whereas $J(q) \in \mathbb{R}^{6 \times n}$ is the robot Jacobian and $\tau \in \mathbb{R}^n$ the control input vector of the robot force control. The input torque vector τ was therefore imposed, exploiting the low level Franka Emika Panda torque controller, as

$$\tau = \hat{g}(q) + J^T(q)\vec{F}_{app}^R \quad (6)$$

where $\hat{g}(q) \in \mathbb{R}^n$ represents the real-time estimation of the gravity term available from the manipulator’s internal controller, and $\vec{F}_{app}^R \in \mathbb{R}^6$ is the force applied by the robot on the subjects’ forearm – whose module is equal to the reference force module F_{robot} – expressed in robot base frame coordinates.

III. EXPERIMENT

In order to assess the feasibility of the proposed sEMG-based control, a concept validation experiment was carried

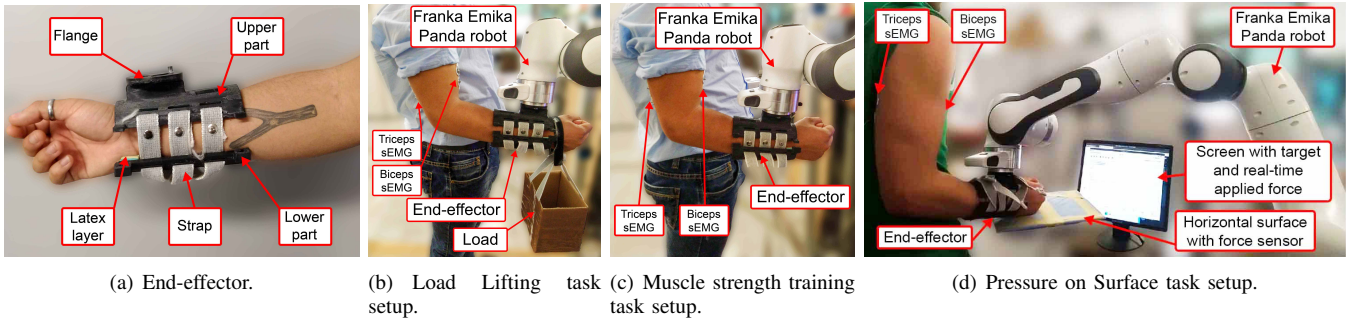


Fig. 5. Experimental setup of the experiments.

out involving four subjects¹ – named U_1, U_2, U_3, U_4 – in a series of physical and muscle strength training tasks. To this aim, we defined the following feasibility criteria on which the concept validation experiment focuses: (i) the ability to limit the sEMG below a specified activity level during the execution of the physical tasks (i.e. a target effort compensation), and (ii) the capacity to bring up the sEMG above a prescribed activity value during the muscle strength training tasks (i.e. a target effort generation.) Furthermore, by this feasibility test, we also report a preliminary assessment of the subjective perceived exertion and usefulness/usability of the overall system through a questionnaire (see Subsec. III-C.2 and Tab. II.)

A. Experimental Task Description and Protocol

In the following, the protocols of the experimental tasks “Load Lifting”, “Pressure on Surface” and “Muscle Strength Training” are illustrated.

1) *Load Lifting Task*: In this task, the subjects started with their forearm flexed by an elbow angle of 90° , with a load applied in proximity of the wrist by means of a small basket equipped with a flexible bracelet, as can be observed in Fig.5(b). In total, two sessions were carried, one with a $1kg$ load and the other with a $2kg$ load. At the beginning of the task the assistive control is turned off. After approximately 5–10s, the sEMG-based control was activated, enabling the robot to start provide assistance to the subject. At this point, the subjects were asked to wait with the elbow flexed at 90° for about 5s, and then to start performing 8 forearm extension-flexion motions, covering the elbow angle range between approximately 90° and 10° , and performing smooth and reasonably slow movements.

2) *Pressure on Surface Task*: During this kind of task, the subjects was required to press with their forearm on a horizontal surface, in order to apply a target vertical force by using only the elbow joint. The related experimental setup can be observed in Fig. 5(b). The horizontal surface was mounted as the end-effector of a second robot manipulator, so that a location adjustment with respect to the height and body of each subject was possible. The surface was therefore located approximately $10cm$ below the wrist of the subjects when their forearm was flexed by 90° . Importantly,

the horizontal surface was equipped with a force sensor (ATI Multi-axis Force/Torque Sensor System ISA F/T-16), and a screen was placed in front of the subjects, in order to provide them with a visually instructed value of pressure force (see again Fig. 5(c).) In particular, two experimental sessions for each subject were performed, related to the application of a vertical force on the surface of $25N$ and $35N$. At the beginning, the subjects were required to apply the pressure force level instructed on the screen without robot assistance and then, after approximately 15s, the assistive control was activated: the subjects were therefore asked to continue provide the same pressure force.

3) *Muscle Strength Training Task*: The procedure of this task consisted in the subjects starting in the 90° elbow flexed configuration, with the assistive control deactivated. After approximately 10s, the control was turned on. II-B.1. For about 10 additional seconds, the user is required to keep the elbow flexed at 90° , and after that, to perform 8 forearm extension-flexion motions, in a continuous and smooth manner in the covering the range between 90° and 10° of the elbow. This task was repeated for two sessions: one for the effort generation of the biceps muscle and the other for the triceps muscle.

B. Selection of the Threshold Values

For the Load Lifting and Pressure on Surface physical tasks, the biceps’ and triceps’ sEMG signals were acquired for 10s in a calibration recording E_C , while the subject was keeping the forearm flexed at an elbow angle of 90° with a load of $1kg$ applied at the wrist. Thereafter, the thresholds were computed as

$$\begin{aligned} T_{2,b} &= \mu_{C,b} - \sigma_{C,b}, & T_{1,b} &= 2T_{2,b}/3, \\ T_{1,t} &= \mu_{C,t} + \sigma_{C,t}, & T_{2,t} &= 3T_{1,t}/2. \end{aligned} \quad (7)$$

where $\mu_{C,b}, \mu_{C,t}$ are the mean values of the biceps’ and triceps’ sEMG calibration recording E_C , and $\sigma_{C,b}, \sigma_{C,t}$ are the standard deviations computed over the same recording. Differently, for the Muscle Strength Training tasks a calibration recording E_R of the biceps’ and triceps’ sEMG was acquired with the forearm flexed at 90° without any load applied. The thresholds were therefore computed as

$$\begin{aligned} T_{2,b} &= \mu_{R,b} + \sigma_{R,b}, & T_{1,b} &= 3T_{2,b}/2, \\ T_{2,t} &= \mu_{R,t} + \sigma_{R,t}, & T_{1,t} &= 3T_{2,t}/2. \end{aligned} \quad (8)$$

where $\mu_{R,b}, \mu_{R,t}$ and $\sigma_{R,b}, \sigma_{R,t}$ are the mean values and the standard deviations over the calibration recording E_R .

¹We engaged four healthy participants (males, right-handed, age: 30.5 ± 4). The experiments were performed in accordance with the Declaration of Helsinki and all participants were thoroughly informed about the experimental protocol and were asked to sign an informed consent form.

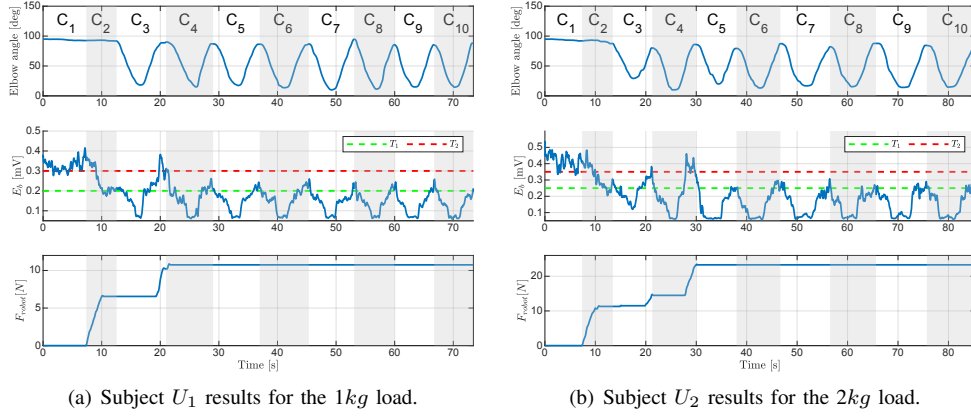


Fig. 6. Single-subject results for the Load Lifting task. E_i represents the sEMG signal, F_{app} the control-driven assistive force of the robot, and $T_{1,i}$ and $T_{2,i}$ the threshold values for the DTS_i block and related FSM (refer also to Sec. II-B, Fig. 1, Fig. 2) – with $i = \{b, t\}$ indicating biceps and triceps. C_1, C_2, \dots, C_{10} divide the task in temporal portions.

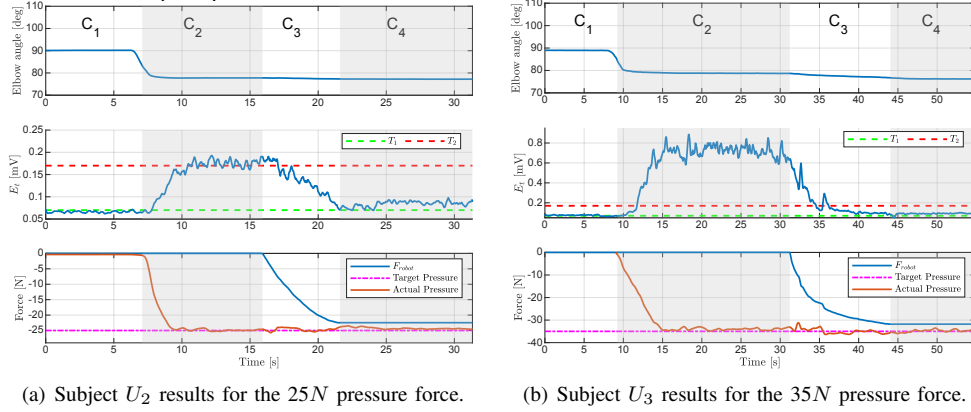


Fig. 7. Single-subject results for the Pressure on Surface task. For the variables meaning refer to the caption of Fig. 6.

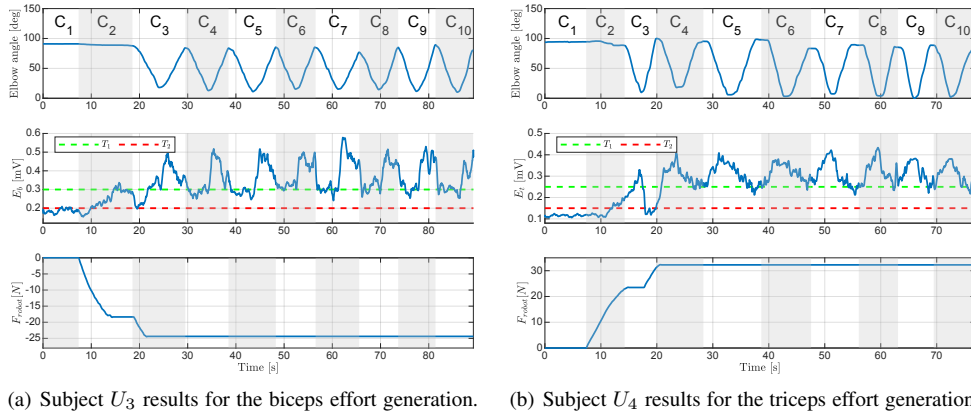
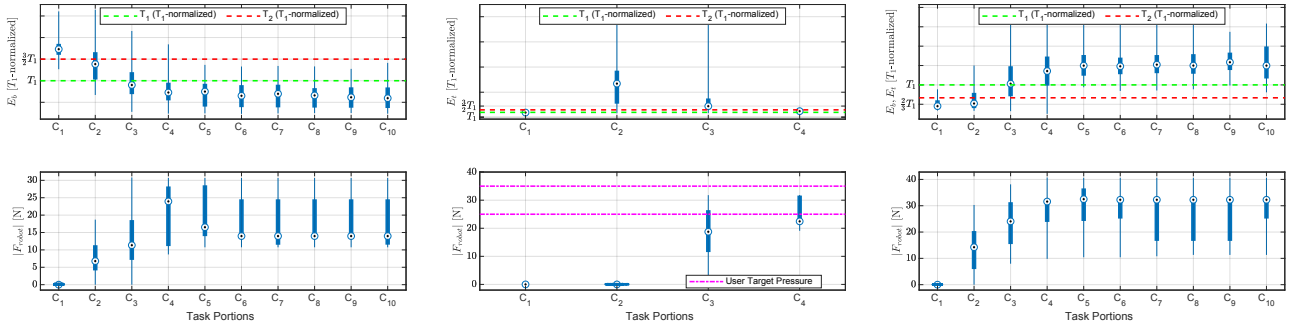


Fig. 8. Single-subject results for the Muscle Strength Training task. For the variables meaning refer to the caption of Fig. 6.

TABLE II

SUBJECTIVE EVALUATION OF THE ROBOTIC ASSISTANCE. THE REPORTED SCORES ARE REPORTED IN RELATION TO A SEVEN POINT LIKERT SCALE FROM 1 (ENTIRELY DISAGREE) TO 7 (ENTIRELY AGREE), AND A 6 (NONE) TO 20 (VERY, VERY HARD) BORG SCALE OF PERCEIVED EXERTION.

Outcome type	Physical Tasks	Average Score	Muscle Strength Training	Average Score
Perceived usefulness	PU1 <i>The robotic assistance was useful during the task executions.</i>	6.5 (Likert)	<i>The robotic assistance was useful for the muscle effort generation.</i>	6.5 (Likert)
	PU2 <i>The robotic assistance reduced my effort during the task executions.</i>	7 (Likert)	<i>The robotic assistance made my muscular effort increase during the motion executions.</i>	7 (Likert)
	PU3 <i>During the robotic assistance, I was able to perform desired motions to execute the tasks.</i>	6.5 (Likert)	<i>During the robotic assistance, I was able to perform the desired motions.</i>	7 (Likert)
Perceived ease of use	PEU1 <i>It was easy to exploit the robotic assistance during the tasks.</i>	6.75 (Likert)	<i>It was easy to exploit the robotic assistance for the effort generation.</i>	6.25 (Likert)
	PEU2 <i>It was intuitive to exploit the robotic assistance during the task executions.</i>	6.75 (Likert)	<i>It was intuitive to exploit the robotic assistance for the effort generation.</i>	6.25 (Likert)
Emotions	E1 <i>I liked to receive the robotic assistance.</i>	6.75 (Likert)	<i>I liked to receive the robotic assistance.</i>	6.25 (Likert)
Comfort	C1 <i>I felt comfortable in exploiting the robotic assistance.</i>	6.75 (Likert)	<i>I felt comfortable in exploiting the robotic assistance for the effort generation.</i>	6.25 (Likert)
Perceived Exertion (Borg Scale)		9 (Very Light)	Perceived Exertion (Borg Scale)	14 (Somewhat Hard)



(a) Aggregated results for the Load Lifting task. (b) Aggregated results for the Pressure on Surface task. (c) Aggregated results for the Muscle Strength Training task.

Fig. 9. Global results of the experimental tasks over the four subjects. With $i = \{b, t\}$ indicating biceps and triceps, E_i represents the sEMG signal, F_{app} the control-driven assistive force of the robot, and T_1 and T_2 the normalized threshold values.

C. Results

Firstly, single-subject results are reported. Secondly, the results are presented in an aggregated manner over the four subjects.

1) *Single-Subject Results*: Referring to Fig. 6, it is possible to observe the temporal plots of the elbow motion (top graph), biceps sEMG signal E_b (middle graph) and sEMG-driven support force F_{robot} (bottom graph) – refer also to Fig. 1 – related to the Load Lifting task. In particular, Fig. 6(a) is related to the effort compensation modality for the $1kg$ load and Fig. 6(b) for the $2kg$ load, related to the subjects U_1 and U_2 , respectively. Note that, in those graphs, 10 temporal portions of the tasks have been highlighted and labeled as C_1, C_2, \dots, C_{10} . For both subjects of Fig. 6, it is possible to observe that at the beginning of the task (portion C_1) the sEMG-based control was turned off and the robot didn't provide any assistive force (portion C_1 , $F_{robot} = 0$), and that the biceps' muscular activity E_b was surpassing the threshold value $T_{2,b}$. Thereafter, at the start of the task portion C_2 the assistive control was activated: in this way, the activity E_b decreased until to reach the threshold value $T_{1,b}$. Then, the subjects started the continuous forearm extension-flexion motions. After one flexion-extension motions for the subject U_1 (task portion C_3) and 2 flexion-extension motions for the subject U_2 (task portions C_3, C_4), the muscular activity E_b was limited to the neighbourhood of the threshold $T_{1,b}$, without surpassing the threshold value $T_{2,b}$ for the rest of the flexion-extension motions of the task, showing that the effort compensation was successfully provided.

Referring now to Fig. 7, the effort compensation results for the Pressure on Surface task are reported for the subjects U_2 and U_3 , in relation to the application of a $25N$ (Fig. 7(a)) and $35N$ (Fig. 7(b)) pressure force, respectively. In the portion C_2 the subjects started to apply the force on the surface, in order to exert the visually instructed target force value of $25N$ or $35N$ (this target force was shown to the subjects on a screen, together with the real time plot of the applied force, see Fig. 5(d) and Subsec. III-A.) After approximately $15s$ the control system was activated, in the task portions C_3 and C_4 : F_{robot} started to increase, causing the decreasing of E_t until it reached the threshold value $T_{1,t}$, causing the stabilization of F_{robot} to the level required for the task/user. Indeed, for the last task portion C_4 , E_t is limited to a the neighborhood

of the the threshold $T_{1,t}$ without exceed $T_{2,t}$.

Fig. 8 reports the assistive behaviour during the Muscle Strength Training task. In particular, the effort generation results for the biceps are reported in Fig. 8(a) for the subject U_3 , and for the triceps in Fig. 8(b) for the subject U_4 . Referring to Fig. 8(a) and 8(b), in the task portion C_2 , the HITL control was turned on, and the robot consequently increased the assistive force provided to the subjects. Indeed, in the portion C_2 , the signals E_b and E_t increased until they reached the threshold value $T_{1,b}$ and $T_{1,t}$, causing the stop of the increasing of F_{robot} . Thereafter, for each task portion from C_3 to C_{10} , the subjects performed the already explained continuous extension-flexion forearm motions. In a similar manner to the behaviour observed for the Load Lifting task, only one extension-flexion iteration was necessary to generate the necessary support force, as can be observed by looking at E_b (Fig. 8(a)) and E_t (Fig. 8(b)).

2) *Global Results*: In Fig. 9, the results of the robot assistance are globally reported over the four subjects for Load Lifting, Pressure on Surface and Muscle Strength Training. Note that the goal of Fig. 9 is to present the results of all subjects in a compact manner, and not to prove statistical significance of the data. In order to make the data related to the muscular activity comparable among the different subjects and experimental sessions, the sEMG signals (and the threshold values) of each subject are normalized with respect to the subject/task-related threshold value $T_{1,i}$. Fig. 9(a) reports the aggregated results of the Load Lifting task, for both the $1kg$ and $2kg$ load cases. Looking at the top graph of this figure, it is possible to observe that from the activation of the assistive control in the portion C_2 , it is visible a clear descending trend of E_b (and increasing trend of $|F_{robot}|$), and from the portions C_5 onward the biceps sEMG activity was bounded above by a small neighborhood of the threshold $T_{1,b}$ without surpassing $T_{2,b}$. Also the global results of Fig. 9(b) confirm for all subjects the assistive behaviour of the single-subjects results, in this case related to the Pressure on Surface task. Indeed, it is possible to observe how the triceps sEMG of all subjects was limited to the threshold $T_{1,t}$ in the task portion C_4 . Fig. 9(c) reports the results for the effort generation experiments. It is clear how the sEMG activity of all subjects (E_b or E_t) was bounded below by a neighborhood of the threshold $T_{1,i}$.

Therefore, the validation concept experiment reported for positive outcomes on the feasibility of the proposed HITL control. In particular, it was demonstrated for all subjects the ability of the system to impose an sEMG upper limit during physical tasks and an sEMG lower limit during muscle strength training tasks. This was successfully realized satisfying for all subjects specified muscular activity levels, in accordance to the feasibility criteria previously outlined in this section. Lastly, Tab. II reports the results of a questionnaire for a simple qualitative assessment of the subjective perceived exertion and usability/acceptance of the robotic assistance. The questionnaire is composed by a customized version of the Questionnaire for the Evaluation of Physical Assistive Devices (QUEAD) [20], evaluating the outcomes Perceived Usefulness (PU), Perceived Ease of Use (PEU), Emotions (E) and Comfort (C). The subjects rated seven statements (Tab. II) on a seven point Likert scale: 1 (entirely disagree), 2 (mostly disagree), 3 (somewhat disagree), 4 (neither agree nor disagree), 5 (somewhat agree), 6 (mostly agree), 7 (entirely agree.) All the average scores computed over the subjects were greater than 6, as reported in Tab. II, showing a positive evaluation on the overall system in terms of a subjective feedback on usefulness and usability. Furthermore, the results related to the perceived exertion (Boerg Scale of Perceived Exertion [21]), confirm a coherent robotic assistance during physical and muscle strength training tasks. Therefore the outcomes provide promising perspectives for future studies in which the proposed robot control can be applied to a given end-user population for assistive and rehabilitation purposes.

IV. CONCLUSIONS

In this work we have presented a sEMG based assistive control for physical tasks and muscle strength training. The proposed HITL control was based on biceps/triceps sEMG signals, without the usage of joint torque estimation methods, with the aim of achieving both muscular effort compensation and generation. The designed control strategy have been evaluated in a concept validation experiment composed by both physical and muscle strength training tasks. The reported results show the feasibility of proposed method by means of both single-subject and global analyses, and a preliminary assessment of subjective usability and usefulness on the overall system has been reported using a questionnaire. These positive outcome lays the groundwork for future research in which the designed sEMG-based HITL control can be applied in assistive and rehabilitation applications, involving both healthy and impaired subjects. Future studies will also focus on improving the control for multi-DoF activities and co-contraction scenarios. In particular, we think that the scaling of the proposed control for a multi-DoF experiment will require a series a further investigations. A quantitative assistance for multi-DOF elbow activities is a very challenging problem, and we will devote future work – both short and long term research – to favour the integration of different studies, such as: multi-DoF human kinematics and muscle activation understanding, human motion intent detection and

closed-loop sEMG-driven control.

REFERENCES

- [1] J. L. Pons, *Wearable robots: biomechatronic exoskeletons*. John Wiley & Sons, 2008.
- [2] C. Yang, J. Zhang, Y. Chen, Y. Dong, and Y. Zhang, "A review of exoskeleton-type systems and their key technologies," *Proceedings of the Institution of Mechanical Engineers, Part C: Journal of Mechanical Engineering Science*, vol. 222, no. 8, pp. 1599–1612, 2008.
- [3] L. Ada, S. Dorsch, and C. G. Canning, "Strengthening interventions increase strength and improve activity after stroke: a systematic review," *Australian Journal of Physiotherapy*, vol. 52, no. 4, pp. 241–248, 2006.
- [4] L. Bowker, J. Price, and S. Smith, *Oxford handbook of geriatric medicine*. OUP Oxford, 2012.
- [5] R. A. Donatelli and M. J. Wooden, *Orthopaedic Physical Therapy-E-Book*. Elsevier health sciences, 2009.
- [6] J. Iruthayarajah, M. Mirkowski, M. M. O. Reg, N. Foley, A. Iliescu, S. Caughlin, J. Harris, S. Dukelow, J. Chae, J. Knutson *et al.*, "Upper extremity motor rehabilitation interventions," 2019.
- [7] M. M. Ditmyer, R. Topp, and M. Pifer, "Prehabilitation in preparation for orthopaedic surgery," *Orthopaedic Nursing*, vol. 21, no. 5, pp. 43–54, 2002.
- [8] H. S. Lo and S. Q. Xie, "Exoskeleton robots for upper-limb rehabilitation: State of the art and future prospects," *Medical engineering & physics*, vol. 34, no. 3, pp. 261–268, 2012.
- [9] T. Lenzi, S. M. De Rossi, N. Vitiello, and M. C. Carrozza, "Proportional EMG control for upper-limb powered exoskeletons," *Proceedings of the Annual International Conference of the IEEE Engineering in Medicine and Biology Society, EMBS*, pp. 628–631, 2011.
- [10] L. Bi, C. Guan *et al.*, "A review on emg-based motor intention prediction of continuous human upper limb motion for human-robot collaboration," *Biomedical Signal Processing and Control*, vol. 51, pp. 113–127, 2019.
- [11] C. Fleischer and G. Hommel, "A human–exoskeleton interface utilizing electromyography," *IEEE Transactions on Robotics*, vol. 24, no. 4, pp. 872–882, 2008.
- [12] W. Hassani, S. Mohammed, and Y. Amirat, "Real-time emg driven lower limb actuated orthosis for assistance as needed movement strategy," 2013.
- [13] T. Teramae, T. Noda, and J. Morimoto, "Emg-based model predictive control for physical human–robot interaction: Application for assist-as-needed control," *IEEE Robotics and Automation Letters*, vol. 3, no. 1, pp. 210–217, 2017.
- [14] L. Peternel, T. Noda, T. Petrič, A. Ude, J. Morimoto, and J. Babič, "Adaptive control of exoskeleton robots for periodic assistive behaviours based on emg feedback minimisation," *PloS one*, vol. 11, no. 2, p. e0148942, 2016.
- [15] S. Mghames, C. D. Santina, M. Garabini, and A. Bicchi, "A neuromuscular-model based control strategy to minimize muscle effort in assistive exoskeletons," *IEEE International Conference on Rehabilitation Robotics*, vol. 2019-June, pp. 963–970, 2019.
- [16] R. Meattini, M. Hosseini, G. Palli, and C. Melchiorri, "Early evaluation of semg-driven muscle modelling for rehabilitation and assistive applications based on wearable devices," in *2016 IEEE International Conference on Robotics and Biomimetics (ROBIO)*. IEEE, 2016, pp. 1480–1485.
- [17] S. Benatti, B. Milosevic, F. Casamassima, P. Schönle, P. Bunjaku, S. Fateh, Q. Huang, and L. Benini, "Emg-based hand gesture recognition with flexible analog front end," in *2014 IEEE Biomedical Circuits and Systems Conference (BioCAS) Proceedings*. IEEE, 2014, pp. 57–60.
- [18] F. Emika, "Panda," Accessed 2017-10-06.[Online]. Available: <https://www.franka.de>, Tech. Rep., 2018.
- [19] B. Siciliano, L. Sciacivico, L. Villani, and G. Oriolo, *Robotics: modelling, planning and control*. Springer Science & Business Media, 2010.
- [20] J. Schmidler, K. Bengler, F. Dimeas, and A. Campeau-Lecours, "A questionnaire for the evaluation of physical assistive devices (quead): Testing usability and acceptance in physical human-robot interaction," in *2017 IEEE International Conference on Systems, Man, and Cybernetics (SMC)*. IEEE, 2017, pp. 876–881.
- [21] G. Borg, "Perceived exertion as an indicator of somatic stress," *Scandinavian journal of rehabilitation medicine*, 1970.